Special Issue Article

Advances in Mechanical Engineering

Advances in Mechanical Engineering
2015, Vol. 7(6) 1–14

DOI: 10.1177/1687814015589464
aime.sagepub.com
SAGE

Influence of apparent wave velocity on seismic performance of a super-long-span triple-tower suspension bridge

Hao Wang[1], Jian Li[2], Tianyou Tao[1], Chunfeng Wang[1] and Aiqun Li[1]

Abstract

As one of the main characteristics of seismic waves, apparent wave velocity has great influence on seismic responses of long-span suspension bridges. Understanding these influences is important for seismic design. In this article, the critical issues concerning the traveling wave effect analysis are first reviewed. Taizhou Bridge, the longest triple-tower suspension bridge in the world, is then taken as an example for this investigation. A three-dimensional finite element model of the bridge is established in ABAQUS, and the LANCZOS eigenvalue solver is employed to calculate the structural dynamic characteristics. Traveling wave effect on seismic responses of these long-span triple-tower suspension bridges is investigated. Envelopes of seismic shear force and moment in the longitudinal direction along the three towers, relative displacements between the towers and the girder, and reaction forces at the bottoms of the three towers under different apparent wave velocities are calculated and presented in detail. The results show that the effect of apparent wave velocity on the seismic responses of triple-tower suspension bridge fluctuates when the velocity is lower than 2000 m/s, and the effects turn stable when the velocity becomes larger. In addition, the effects of traveling wave are closely related to spectral characteristics and propagation direction of the seismic wave, and seismic responses of components closer to the source are relatively larger. Therefore, reliable estimation of the seismic input and apparent wave velocity according to the characteristics of the bridge site are significant for accurate prediction of seismic responses. This study provides critical reference for seismic analysis and design of long-span triple-tower suspension bridges.

Keywords

Apparent wave velocity, seismic performance, triple-tower suspension bridges, non-uniform ground motion, propagation direction

Date received: 8 June 2014; accepted: 26 December 2014

Academic Editor: Weidong Zhu

Introduction

The issue of multi-support seismic excitation (MSE) for civil infrastructures is mainly due to the traveling wave effect, incoherence effect, and site-response effect of seismic waves. Deterministic dynamic method in time domain or frequency domain[1–3] and random vibration method[4–6] are the two widely adopted approaches to analyze the MSE problems.[7] However, further studies are required for practical applications of the above two methods in that they are still facing some problems.

[1]Key Laboratory of Concrete and Prestressed Concrete Structure of Ministry of Education, Southeast University, Nanjing, China
[2]Department of Civil, Environmental and Architectural Engineering, The University of Kansas, Lawrence, KS, USA

Corresponding author:
Hao Wang, Key Laboratory of Concrete and Prestressed Concrete Structure of Ministry of Education, Southeast University, No. 2 Sipailou, Nanjing 210096, China.
Email: wanghao1980@seu.edu.cn

The traditional deterministic dynamic methods have been used broadly; however, it cannot consider the random characteristics of ground motion. As for the random vibration method, it is time-consuming since too much random factors are included during the structural seismic analysis. Consequently, the investigation on combined influences of the two above-mentioned methods on structural responses was also conducted.[8,9] As one of the contributors to MSE, traveling wave effect appears more and more significant for long-span bridges when the bridge span increases. For suspension bridges, traveling wave effect could impose higher seismic demand to these bridges and therefore should be taken into account.[10–13]

Among the above methods that deal with MSE problems, the deterministic dynamic analysis in time domain can provide the entire structural response in time domain during a certain earthquake. Therefore, it could be employed to investigate the effects of traveling wave for a specific earthquake on structures. A great deal of research has been focused on the effect of MSE on long-span bridges.[14–16] Unfortunately, there are still no conclusive conclusions about the effects of traveling wave on long-span bridges at present. In order to perform MSE analysis in time domain, the following issues should be addressed:

1. *Determination of the seismic input points*. Different seismic input has great impacts on structural response under earthquakes. However, there are different views on selecting seismic input points for multi-span bridges. For continuous girder and cable-stayed bridges, it is generally agreed that all pier supports should be selected to apply seismic input. However, whether abutments should be treated the same as piers is still controversial. Similarly, descriptions are often missing that whether anchorages of suspension cables should be considered as sources of seismic input or just fixed boundaries. Peng[17] took anchorages of suspension cables as seismic input when analyzing non-uniform seismic responses of suspension bridges.
2. *Apparent wave velocity*. Evidently, apparent wave velocity will affect the phases among the seismic inputs at various locations of the bridge supports and is therefore a crucial factor to traveling wave effect.[18] Discrepancy or contradictory conclusions may be derived if different velocities are applied to the same structure. Unfortunately, documents about the effects of traveling wave on long-span bridges offer a quite wide range of velocity. Such velocity could be derived from geological survey reports, or a broad range of velocity will be used in the analysis. Many studies even gave no apparent wave velocity or just carried out the calculation using a hypothetical velocity.[9,19] Diverse velocities would lead to suspicious results. Harichandran and Vanmarcke[20] regarded apparent wave velocity as an essentially S-wave and the velocity would keep constant during the propagation, and the following velocities: 4500, 3900, 2800, and 2400 m/s were selected to carry out the calculation. Ates et al.[21] analyzed MSE of a 292.8-m-long continuous girder bridge with velocities being 400, 700, and 1000 m/s, respectively. Soyluk and Dumanoglu[22] considered the velocity value to be dependent on the soil conditions of the bridge site; three different velocity groups were used to calculate the effects of traveling wave on the Jindo bridge of South Korea, and they were (a) 1000 m/s (constant); (b) 1800 m/s (firm soil), 600 m/s (medium soil), and 200 m/s (soft soil); and (c) 800 m/s (firm soil), 400 m/s (medium soil), and 200 m/s (soft soil). It was observed that the variation in velocities due to soil conditions had insignificant effects on the pseudo-static displacements but vital effects on the dynamic behavior of the bridge, and responses obtained from spatially varying ground motion model were generally higher than those from constant apparent wave velocity case. Fan et al.[23] studied seismic responses of the second Nanjing Yangtze River Bridge under traveling wave effect with apparent wave velocity being initially taken as 500 m/s. It was proposed that the lower velocity was practically invalid and the velocity should be generally greater than 1000 m/s, and the seismic response of long-span bridges considering the traveling wave effect would be conservative. Wang et al.[24] carried out response analysis of a 344-m-long bridge to non-uniform earthquake ground motions with the velocity being taken from 100 to 2000 m/s. Xiang[25] thought lower apparent wave velocity (43.3–260 m/s) is helpful to reducing the seismic response of cable-stayed bridges. From the above literature, it is evident that the scope of apparent wave velocity is indeed quite broad and the conclusions are inhomogeneous.
3. *Selection of the coordinate system*. The base of structures will move under earthquake excitation. When evaluating the effects of traveling wave on structures, the structural dynamic responses should be defined clearly by whether they are the absolute or relative values.

It is noted that all the above studies focus on two-tower suspension bridges.[13,26,27] However, the

enormous demand for more long-span bridges recently promotes the development of multi-tower suspension bridges. Among them, triple-tower suspension bridges are most attractive for their ability to effectively reduce the dimension of anchorages and suspension cables and therefore the ability to reduce costs. A triple-tower suspension bridge has two side towers at the end of two main spans, as well as a middle tower between main spans to alleviate the strain of main cables and anchors at two ends of the bridge. Obviously, the configuration of the middle tower is crucial to the performance of the overall structure. On one hand, high rigidity of the middle tower would cause difficulty in the sliding of the two main cables which lead to high internal forces of the middle tower under eccentric vehicle loads; on the other hand, low rigidity will lead to large deformation under eccentric vehicle loads and instability under high wind velocity.

Compared with two-tower suspension bridges, structural characteristics of triple-tower suspension bridges are strikingly different due to the addition of a middle tower and a main span. However, relevant studies for triple-tower bridges are insufficient to date. Yoshida et al.[28] studied the parameters influencing the deformation characteristics of a four-span suspension bridge which has two 2000-m main spans and revealed that the rigidity of the middle tower was the dominant factor controlling excessive deformation. Deng et al.[29] found that the natural frequencies of triple-tower suspension bridges are lower when compared to those of two-tower suspension bridges, and vibrations of the main girder occur first and then followed by vibrations of cables and towers. Triple-tower suspension bridges are special because of the addition of the middle tower, and thus, their seismic response related to traveling wave effect should be studied. However, to the authors' knowledge, very few studies about traveling wave effect on triple-tower suspension bridges have been carried out. In this article, Taizhou Yangtze River Bridge, a triple-tower suspension bridge with the longest main span in the world, is taken as a numerical example to facilitate the study of the effects of traveling wave on triple-tower suspension bridges. A relatively broad range of apparent wave velocities varying from 300 to 7000 m/s are applied to carry out the calculation, in order to uncover the correlation between the apparent wave velocity and the dynamic responses of the bridge. The dynamic characteristics of the bridge attached to various velocities under Tianjin earthquake and El Centro earthquake are presented in detail.

Equilibrium equations for MSE

For a lumped-mass system, the dynamic equilibrium equations in absolute coordinates can be written as[30]

$$\begin{bmatrix} M_{00} & M_{01} \\ M_{10} & M_{11} \end{bmatrix} \begin{bmatrix} \ddot{u}_0 \\ \ddot{u}_1 \end{bmatrix} + \begin{bmatrix} C_{00} & C_{01} \\ C_{10} & C_{11} \end{bmatrix} \begin{bmatrix} \dot{u}_0 \\ \dot{u}_1 \end{bmatrix} + \begin{bmatrix} K_{00} & K_{01} \\ K_{10} & K_{11} \end{bmatrix} \begin{bmatrix} u_0 \\ u_1 \end{bmatrix} = \begin{bmatrix} 0 \\ F \end{bmatrix} \tag{1}$$

where u_0 is the n-vector of displacements of the unconstrained degrees of freedom (DOFs); u_1 is the m-vector of support displacements which means the displacements at the constrained nodes; M_{ij}, C_{ij}, and K_{ij} are the mass, damping, and stiffness matrices associated with those displacements, respectively. Note that the forces F associated with the specified displacements are unknown and can be calculated after u_0 has been evaluated.

In order to solve the above equations, some approaches including direct solution method, relative motion method, and large-mass method are primarily adopted.[31,32] These methods are described as follows.

Direct solution method

Direct solution method, by its name, solves equation (1) directly in absolute coordinate using time-stepping integration. The result is more accurate compared with other methods. Besides, this method can be applied to solve for both linear and nonlinear dynamic behaviors of structures. This method possesses the highest accuracy but consumes the most computation time.

Relative motion method

Relative motion method is another approach which is suitable for structural dynamic analysis of MSE.[33] It is possible to decompose the structural responses into pseudo-static and dynamic displacements in linear domain as

$$u_0 = u_0^s + u_o^d \tag{2}$$

where the pseudo-static displacements u_0^s can be obtained from

$$u_0^s = -K_{00}^{-1} K_{01} u_1 \tag{3}$$

Large-mass method

Some approaches to simplify the relevant calculations are proposed to resolve equation (1), including large-mass method, large-rigidity method, Lagrange multiplier method, and so forth. Among them, the most prevalent method is the large-mass method. This is an approximate method to estimate the dynamic response. The main step for realizing this method is to set a mass element at supports which possess approximately 10^6–10^8 times of the mass of the overall structure. When dealing with the effects of traveling wave on structures,

time-history of acceleration should be converted to time-history of load.

To solve dynamic response of structures related to MSE, ANSYS and SAP2000 employ large-mass method while ABAQUS uses direct solution method. In addition, both acceleration and displacement time-history can be selected as the seismic inputs when the direct solution method is applied.[30] The acceleration input is considered to be better since the existing seismic waves were recorded as the acceleration time-histories. Displacement input could be obtained from integration of acceleration input after baseline correction, or it can also be derived from the target displacement spectrum.

This article aims at investigating the effects of traveling wave on long-span bridges based on ABAQUS platform. During the implicit dynamic analysis, the seismic acceleration input can be exerted directly on the bottom of the structure after the constraints on the corresponding directions are released. The variable step method is adopted when carrying out the direct integration. All the results presented herein are in absolute coordinates.

Bridge description and finite element model

In this study, Taizhou Bridge, the first triple-tower suspension bridge in the world which has the main span larger than 1000 m, is taken as an example. Taizhou Bridge spans across the Yangtze River in Jiangsu Province in China and connects Taizhou City on the north side with Changzhou City on the south side, as shown in Figure 1. The overall layout of the bridge and the cross section of the main girder are schematically shown in Figure 2. The spans of the bridge are 390 m + 1080 m + 1080 m + 390 m. The sag-to-span length ratio of main cables is 1/9 and the lateral distance between the two main cables is 35.8 m. The main girder is the welded streamline flat steel box girder. The two reinforced-concrete side towers are 178 m high, and the irregular steel middle tower is 192 m high. The tapered middle tower is a portal frame in the lateral direction and has an inverted "Y" shape in the longitudinal direction. Lateral supports are installed at joints between the inner wall of the middle tower and the main girder to resist wind loads. Vertical and lateral bearings are installed on the lower cross beams of the side towers. In addition, elastic restraints made of steel stranded wires are employed in the longitudinal direction of the middle tower.

The finite element model of Taizhou Bridge is shown in Figure 3. In this model, spatial beam elements are applied to simulate the main box girder, and the actual cross section characteristics are used to model the cross sections of the girder. Three-dimensional (3D) truss elements with the property of resisting only tension but not compression are adopted to simulate the vertical suspenders and the main cables. The main cables are meshed at the suspending points. Lumped mass elements are added to the model to account for the mass of pavement and railings, but their stiffness contributions are neglected. The nonlinearity of the side cable stiffness due to gravity is approximated by linearized stiffness using the Ernst equation of equivalent modulus of elasticity.[34] The connections between the suspenders and the main girder are realized using rigid elements. Furthermore, spatial beam element is also used to simulate the three towers, and spring element according to the design stiffness is employed to simulate the longitudinal elastic restraints between the lower cross beam of the middle tower and the girder.

According to design, at the side tower locations, the movement of the steel box girder in the lateral, vertical, and rotational directions is coupled with that of the side towers. The main cables are fixed on top of the towers. The bottoms of towers and the ends of the main

Figure 1. Taizhou Bridge.

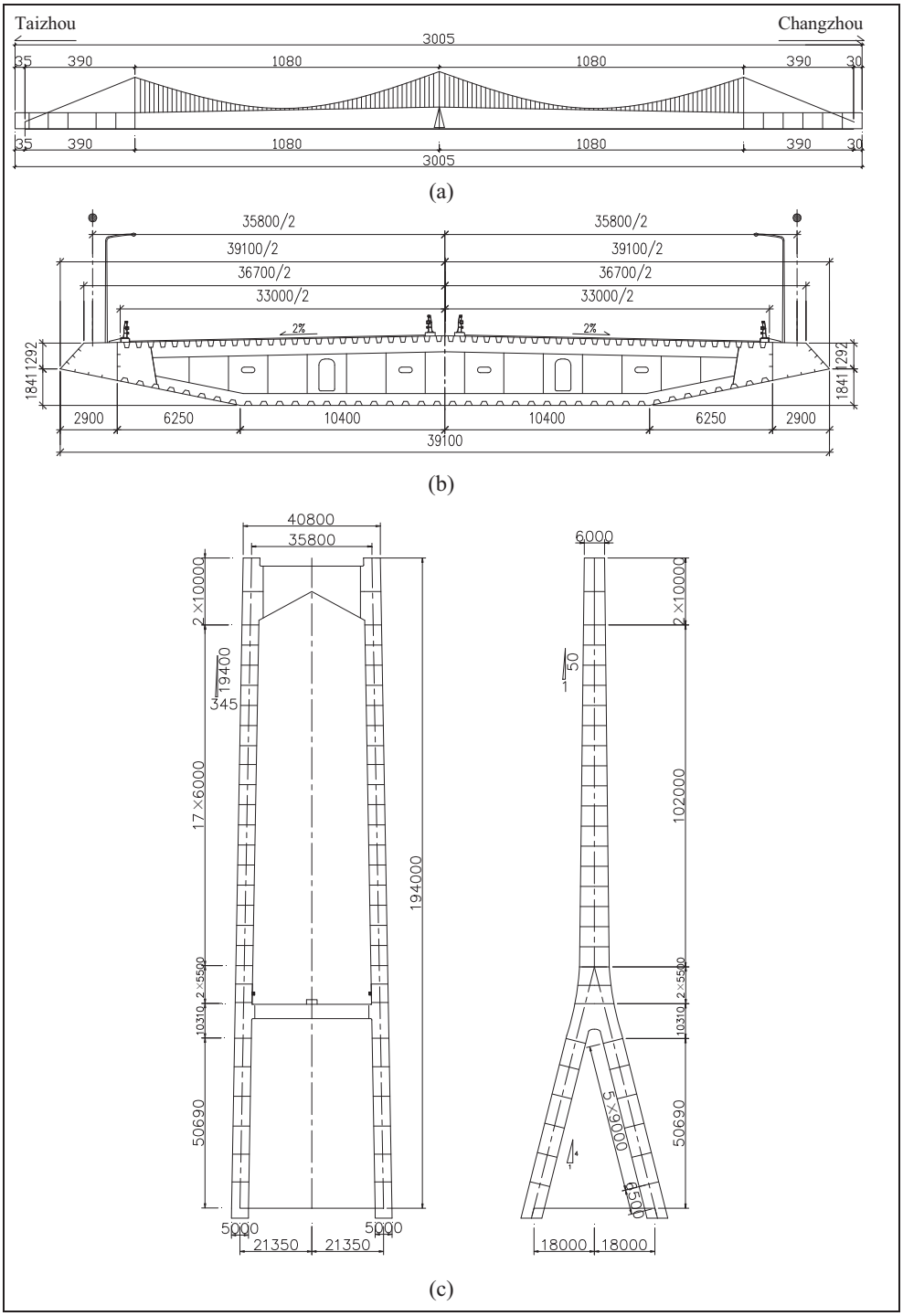

Figure 2. Schematic description of Taizhou Bridge: (a) elevation (m), (b) typical cross section of box girder (cm), and (c) configuration of middle tower (mm).

suspension cables are fixed at the bases. Soil–structure interaction is not considered herein due to the strong pile foundation of Taizhou Bridge.[35]

To reduce the longitudinal displacement of the bridge girder, nonlinear viscous dampers are installed at joints of the lower cross beams and the girder. In this model, the multiple dampers in the same direction are simulated as one damper, and the equivalent force outputs generated by multiple dampers are achieved through alternating the damping coefficient.

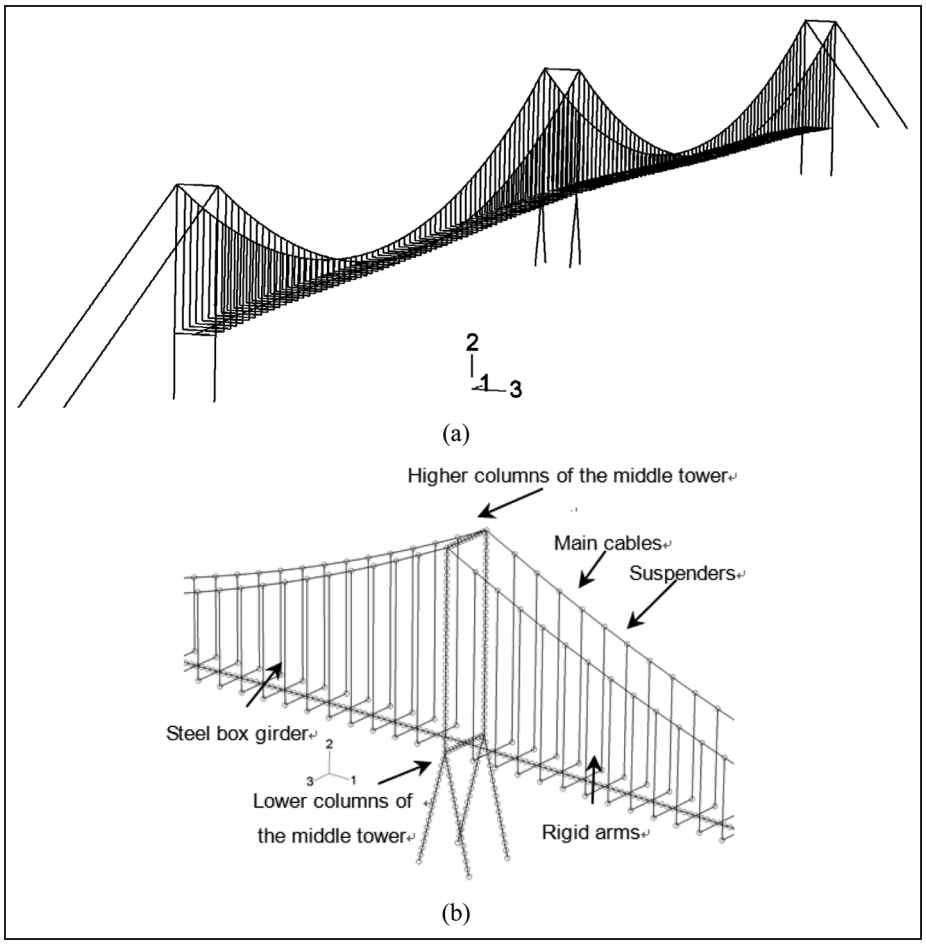

Figure 3. Finite element model of Taizhou Bridge: (a) full finite element model and (b) part of the finite element model.

Seismic responses

Dynamic characteristics of Taizhou Bridge

Structural dynamic characteristics are the basis for seismic response analysis.[36,37] Modal analysis of the bridge is performed considering geometric nonlinearity using LANCZOS eigenvalue solver in ABAQUS. In all, 500 natural frequencies and mode shapes of the bridge are obtained. The first 500 natural frequencies are shown in Figure 4. It is apparent that natural frequencies are concentrated in lower frequency domain below 5 Hz. Moreover, the first 25 natural frequencies are all lower than 0.4 Hz and their mode shapes are described with the corresponding typical features in Table 1. The first eight mode shapes of the bridge are shown in Figure 5.

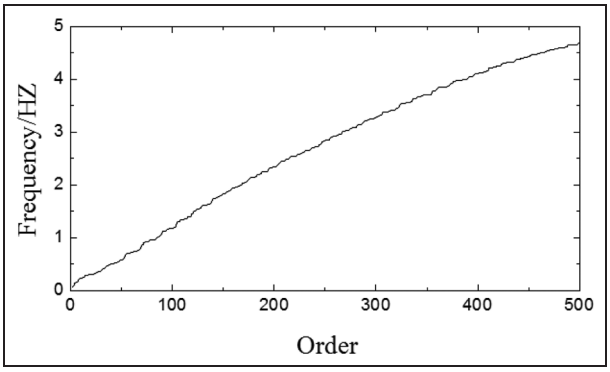

Figure 4. Distribution of the first 500 modal frequencies.

It is generally recognized that the first vibration mode of a two-tower suspension bridge is composed of the symmetric lateral bending deformation of the main girder. However, Table 1 indicates that the first vibration mode of Taizhou Bridge is antisymmetric lateral bending deformation of the steel box girder. The longitudinal floating vibration mode of the bridge girder is not obvious due to the rigid stiffness of the elastic restraint employed between the steel box girder and the middle tower. Besides, all the first 13 mode shapes of Taizhou Bridge are vibrations of the main girder, except the 12th mode which is dominated by the middle tower vibration. The vibration characteristics of Taizhou Bridge in this study coincide with the existing analysis results.[29]

Table 1. First 20 frequencies and mode shapes of the Taizhou Bridge.

Order number	Frequency (Hz)	Mode shape description
1	0.07163	AS L vibration of steel box girder
2	0.08023	AS V vibration of steel box girder
3	0.09512	S L vibration of steel box girder
4	0.11489	AS V vibration of steel box girder
5	0.11758	S V vibration of steel box girder
6	0.13709	S V vibration of steel box girder
7	0.17089	AS V vibration of steel box girder
8	0.18518	S V vibration of steel box girder
9	0.23058	AS L vibration of steel box girder
10	0.23786	AS V vibration of steel box girder
11	0.23983	S V vibration of steel box girder
12	0.24514	L vibration of middle tower
13	0.27290	AS T vibration of steel box girder
14	0.27372	S vibration of main cables
15	0.27377	S vibration of main cables
16	0.28952	S vibration of main cables
17	0.28954	S vibration of main cables
18	0.29015	AS L vibration of main cables
19	0.29064	L vibration of middle tower and main cables
20	0.30262	AS L vibration of main cables
21	0.31461	AS V vibration of towers
22	0.31526	S V vibration of steel box girder
23	0.31831	AS V vibration of steel box girder
24	0.32088	S L vibration of main cables
25	0.36613	S T vibration of steel box girder

S: symmetric; AS: antisymmetric; L: lateral; V: vertical; T: torsional.

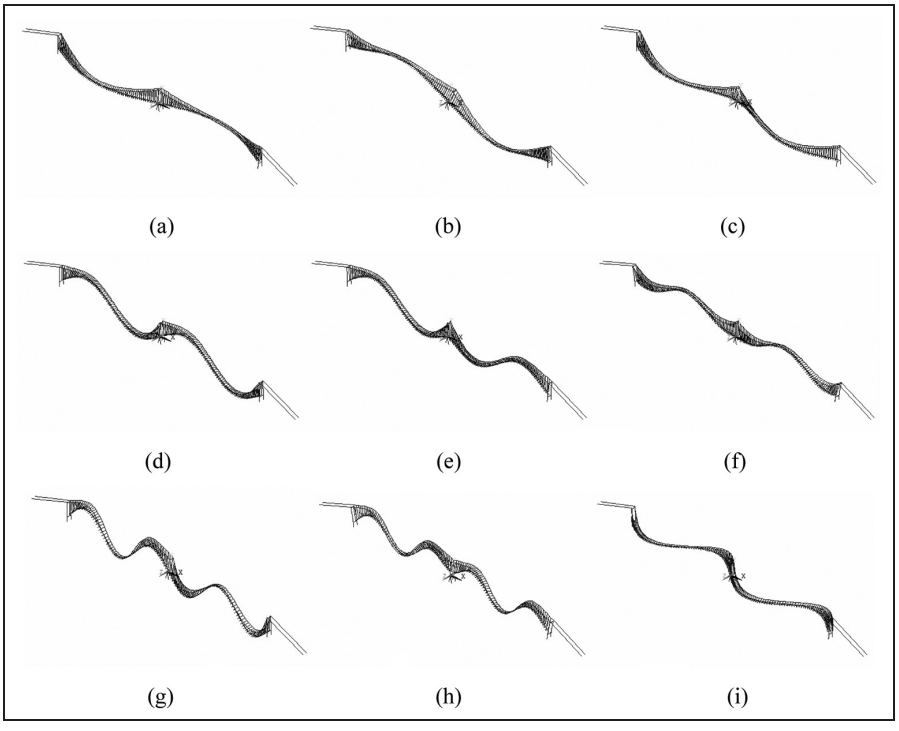

Figure 5. First nine mode shapes of Taizhou Bridge: (a) first mode shape, (b) second mode shape, (c) third mode shape, (d) fourth mode shape, (e) fifth mode shape, (f) sixth mode shape, (g) seventh mode shape, (h) eighth mode shape, and (i) ninth mode shape.

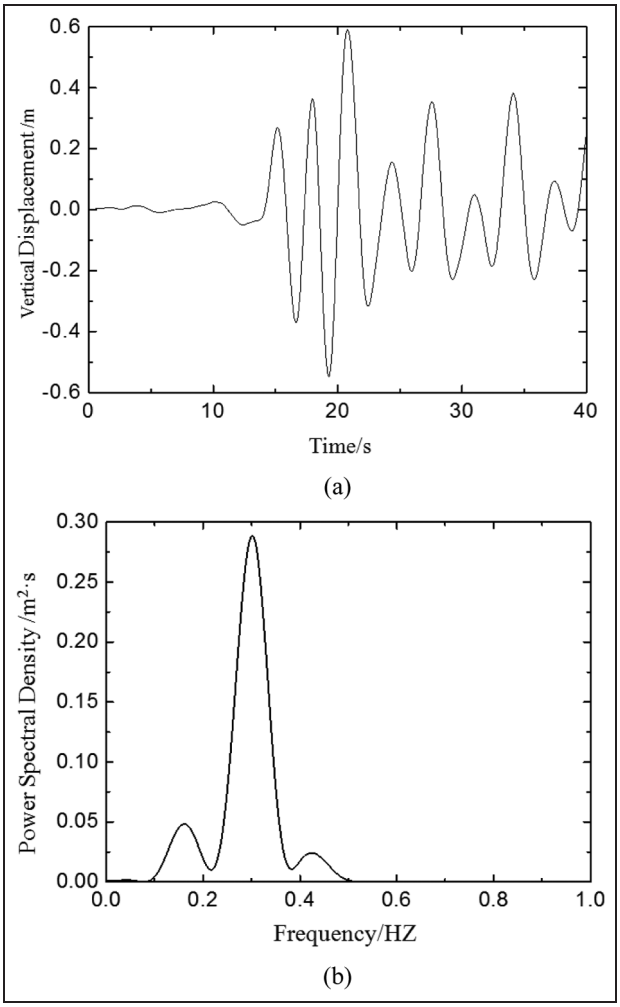

Figure 6. Structural responses at the midspan of Taizhou Bridge under Tianjin earthquake: (a) time-history of vertical displacement and (b) power spectral density.

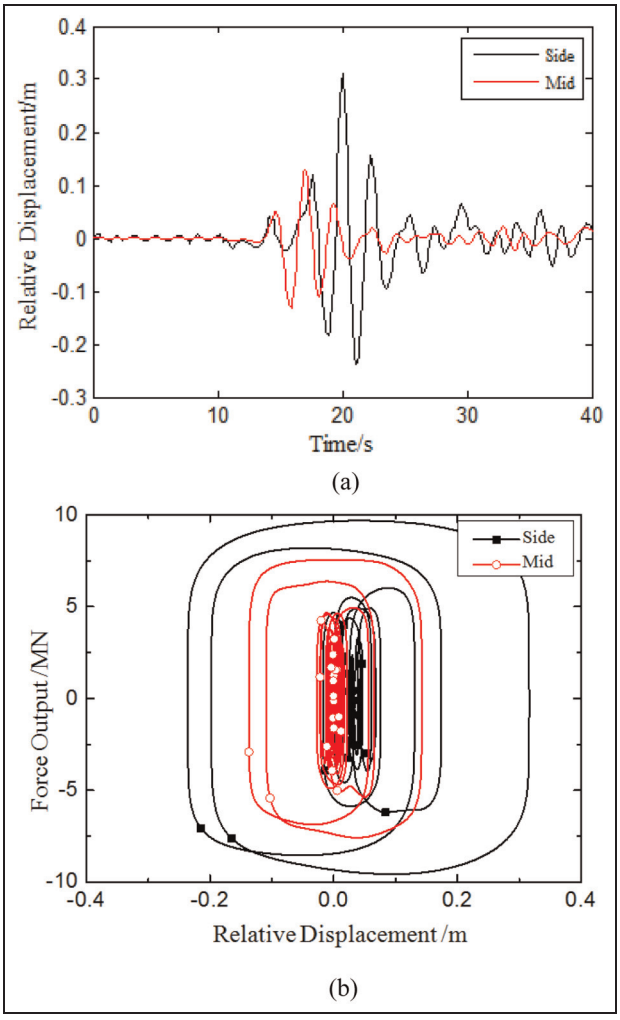

Figure 7. Structural responses of Taizhou Bridge under Tianjin earthquake: (a) relative longitudinal displacement between the tower and the girder and (b) damper hysteresis curve.

Uniform seismic input

In this study, both longitudinal and vertical ground motions are applied. The vertical components are taken as 2/3 of the longitudinal components according to the Chinese design code. The dynamic responses of the bridge under the Tianjin earthquake (with 0.15 g peak acceleration) are presented herein. Tianjin earthquake was recorded at Tianjin Hospital when the earthquake happened in 25 November 1976. The seismic wave was recorded in north–south direction with the time interval of 0.01 s. The magnitude of the earthquake is 6.9 and the measurement station to the epicenter is 65 km. The time-history and the power spectral density (PSD) of the vertical displacement at the midspan of the bridge are shown in Figure 6. The peak value is about 0.6 m in this case. With closer respect to Table 1 and Figure 6, the following conclusions could be obtained: frequencies of the first and second peaks of PSD are close to those of the 7th/8th and 22th/23th natural frequencies, respectively, and the frequency of the third peak is somewhat larger.

When strong earthquake occurs, excessive displacement between side towers and the girder can lead to the falling of the girder, which is one of the main damage scenarios of suspension/cable-stayed bridges under earthquakes.[38] Therefore, a great deal of research has been focused on controlling the relative displacement between the towers and the girder in the longitudinal direction,[27,39,40] which is for simplicity hereafter referred to as the relative displacement. Figure 7 shows the time-history of the relative longitudinal displacement between the towers and the main girder, and the corresponding damper hysteresis curve. The peak value of the relative longitudinal displacement of the main girder at the middle tower is less than those at the side towers, in that the girder is symmetric about the middle

tower and elastic restraints are set between the middle tower and the girder.

Seismic input considering traveling wave effect

There are five input points of seismic excitation in this model: the left anchorage of main cables, the supports of the left tower, the middle tower, and the right tower, and the right anchorage of main cables. The seismic wave propagation direction is assumed from left of the bridge to the right, which means the left tower is closer to the source and time-lagged phenomenon should be considered. Similar to the uniform input case, both longitudinal and vertical ground motions are taken into account and the vertical ground motions are taken as 2/3 of the longitudinal ground motions according to Chinese seismic design specification. Three typical seismic inputs including Tianjin earthquake, El Centro earthquake, and Taft earthquake are analyzed. The results related to Tianjin earthquake and El Centro earthquake (with peak acceleration being 0.15 g) are presented. Due to the lack of geological survey reports at the bridge site, a relatively broad range of apparent wave velocity is employed. The velocity of the apparent wave is taken from 300 to 7000 m/s in this study. The analysis results corresponding to different velocities are labeled in the following diagrams.

Compared with the absolute values, the relative responses have more explicit physical meaning when supports are not fixed. Therefore, relative displacements between the towers and the girder are selected for investigation. The longitudinal shear forces and moments of the left and right towers under Tianjin earthquake are shown in Figures 8 and 9, respectively.

Assuming that each tower is divided into the upper column and lower column by its lower cross beam, it can be concluded from Figures 8 and 9 that (1) dampers installed between the side towers and the girder at the height of 50.69 m would introduce significant changes in the shear force curves and inflection points in the bending moment curves at that height. (2) Bending moments and longitudinal shear forces generated by uniform seismic excitation are greater than those generated by non-uniform seismic excitation. (3) Apparent wave velocity has more influence on shear forces in lower column than those in upper columns. (4) The side tower closer to the source (namely the left tower) would have larger internal forces than the side tower far from the source (namely, the right tower). (5) The shear forces of the upper columns are K-shaped, which means that the shear forces at the top and bottom are larger than the force at the midpoint. The distinction becomes more significant with the increase in apparent wave velocity. (6) The bending moments of the upper columns have parabolic shapes and the moments of the lower columns are approximately linear. The main

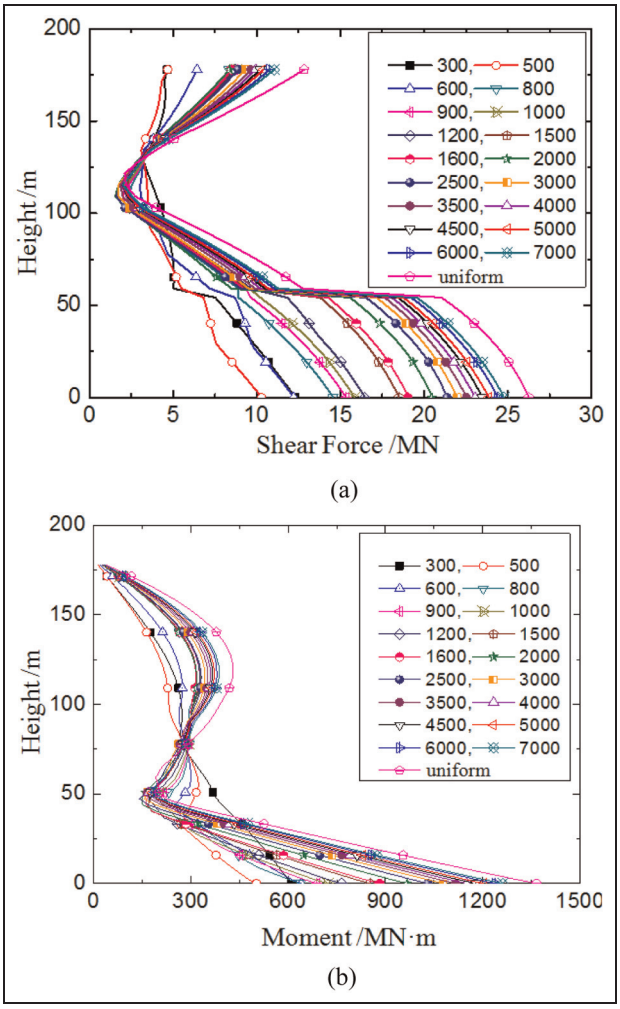

Figure 8. Influences of Tianjin earthquake on the left tower with various apparent wave velocities: (a) longitudinal shear force and (b) longitudinal bending moment.

reason is that the constraint conditions of the upper and lower columns are different. The top of the tower is restrained by the main cable and the base of the tower is fixed on the ground.

The middle tower is an inverted Y-shaped tower in the longitudinal direction, which means that the corresponding stiffness along the bridge is significantly greater than side towers' stiffness. The purpose of the configuration of the middle tower is to offer adequate stiffness to resist the eccentric vehicle loading. Considering the uniqueness of the geometry of the middle tower, the longitudinal shear forces and bending moments of the middle tower under diverse apparent wave velocities are analyzed and are shown in Figure 10. Shear forces of the upper column of the middle tower are also K-shaped and the distribution of the bending moments resembles those of the side towers shown in Figures 8 and 9. The effects of apparent wave velocity of Tianjin earthquake on the longitudinal

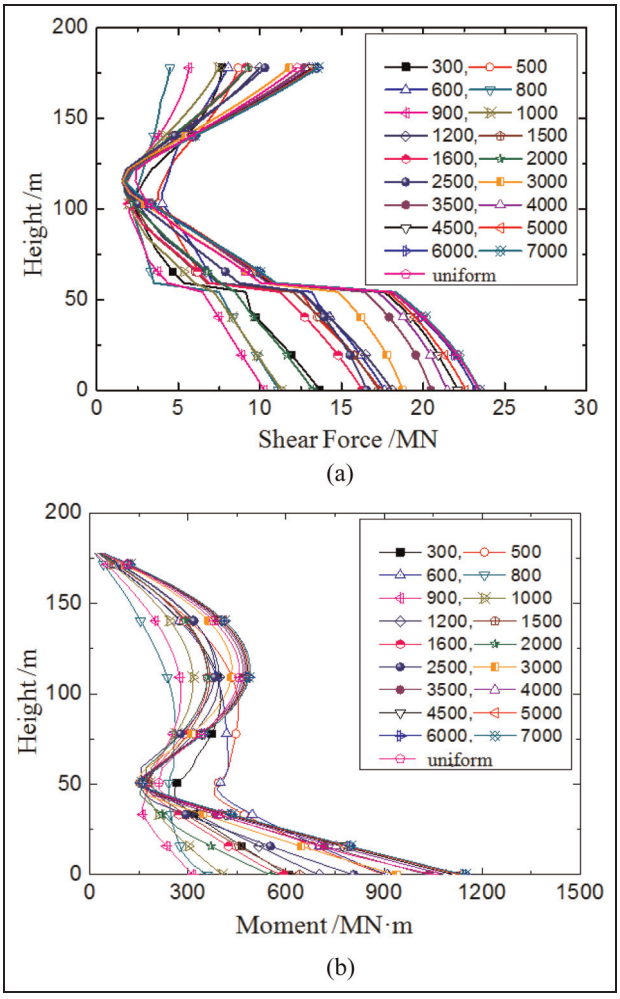

Figure 9. Influences of Tianjin earthquake on the right tower with various apparent wave velocities: (a) longitudinal shear force and (b) longitudinal bending moment.

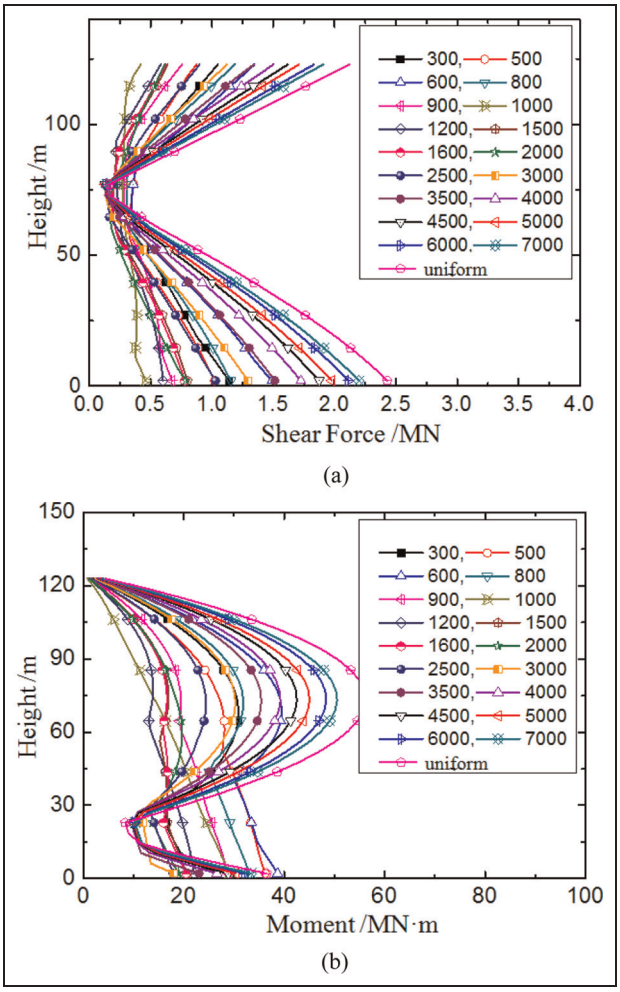

Figure 10. Influences of Tianjin earthquake on the middle tower with various apparent wave velocities: (a) longitudinal shear force and (b) longitudinal bending moment.

shear forces and bending moments at the bottoms of the towers are shown in Figure 11.

As can be seen from Figure 11, the influence of apparent wave velocity of Tianjin earthquake fluctuates when apparent wave velocity is in the lower range (<2000 m/s). Therefore, one has to be cautious when drawing conclusions under low apparent velocities. Shear forces and bending moments at the bottoms of the towers would increase slightly if the velocity exceeds 2000 m/s. Both shear forces and bending moments of the towers closer to the source would be larger than those of the towers far from the source. After the initiation of vibration, dynamic forces of the steel girder are transferred to lower cross beams, and then the forces are passed to the bottoms of towers and anchorages through the main cables, respectively. Because of the relatively larger rigidity of the middle tower and the elastic restraints installed between the middle tower and the girder, shear forces at the bottom of the middle tower are larger than those at the bottoms of the side towers. Meanwhile, the lower middle tower has an inverted Y-shape. Therefore, the vertical loading transferred from the upper tower will be decomposed into vertical and horizontal components, for which the latter part will increase the shear forces at the bottom of the middle tower.

In order to ensure the occurrence of the bridge main girder falling during earthquakes is prevented, the longitudinal relative displacement between the towers and the main girder is analyzed. The influence of the apparent wave velocity on the longitudinal relative displacement in the case of Tianjin earthquake is shown in Figure 12.

Figure 12 indicates that (1) the relative displacement of the tower closer to the source (the left tower) is apparently larger than that of the tower far from the source (the right tower). Therefore, the propagation direction of the earthquake should be specially considered when seismic analysis on a long-span suspension

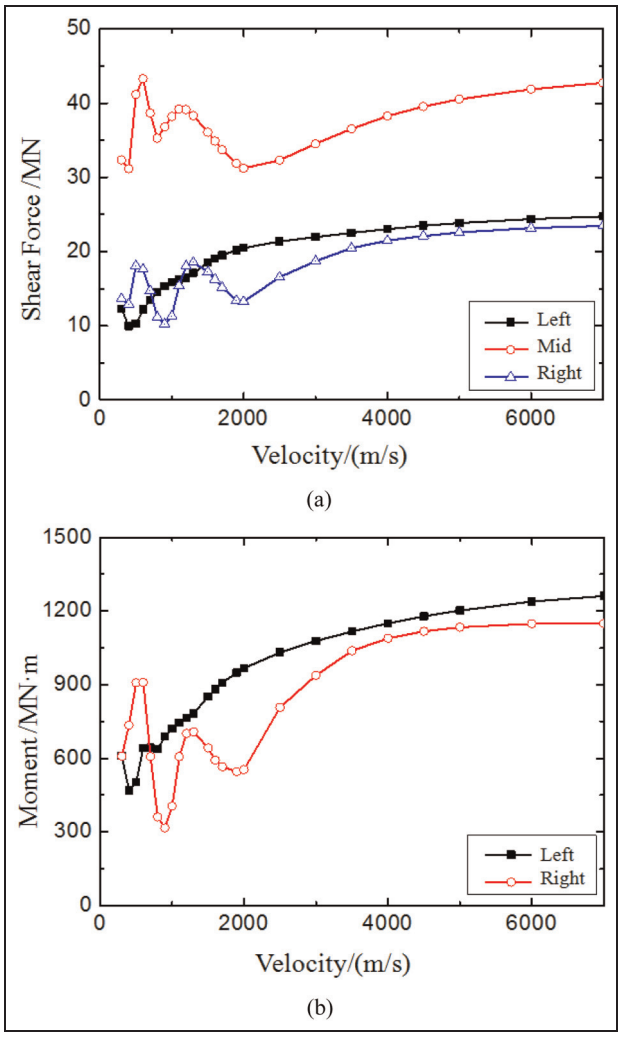

Figure 11. Influences of Tianjin earthquake on the reaction forces at the bottoms of towers with various apparent wave velocities: (a) longitudinal shear force and (b) longitudinal bending moment.

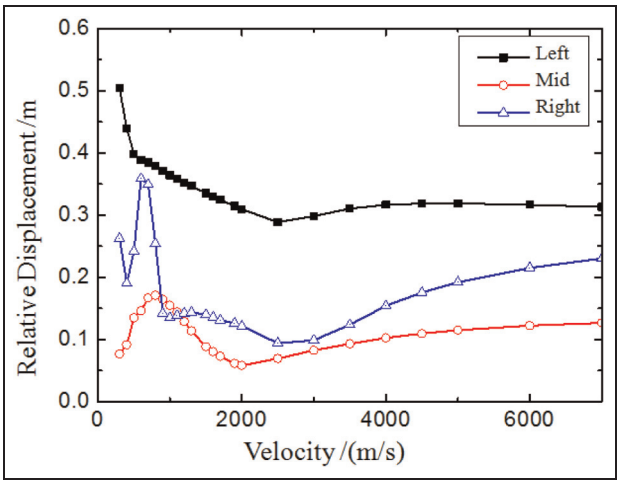

Figure 12. Influences of the apparent wave velocity on the relative displacement between towers and the main girder under Tianjin earthquake.

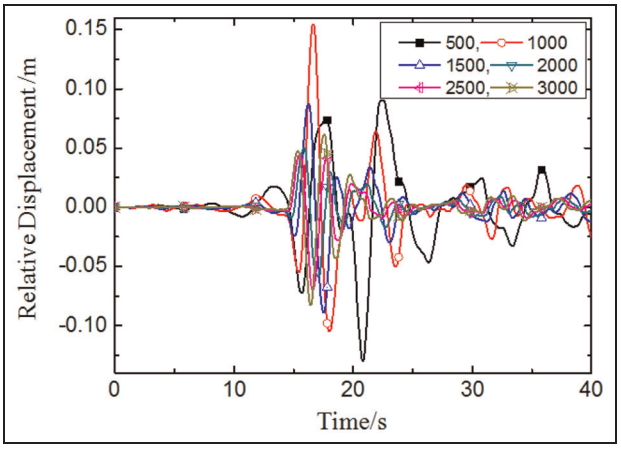

Figure 13. Time-history of relative displacement between towers and the main girder under Tianjin earthquake.

bridge is conducted. (2) Due to the combined function of the viscous dampers and flexible cables at the middle tower, all the three relative displacements are controlled within a certain degree, and the relative displacement at the middle tower is the minimum among the three towers. (3) However, the relative displacement at the left tower is still larger than 0.5 m, which deserves special attention in order to prevent falling of the main girder under earthquake loading. As a few examples, the time-histories of the relative displacement of the middle tower when the apparent wave velocity is below 3000 m/s are shown in Figure 13.

Figures 12 and 13 also show that the relative displacement of the middle tower would increase at first and then decrease as the velocity increases from 800 to 2000 m/s. Moreover, the relative displacement of the left tower shows a sharp decline at the beginning, followed by a slow decline trend and then reaches stabilization with the increase in apparent wave velocity. As to the right tower, the relative displacement oscillates intensively when the velocity is low and then becomes steady.

Unlike the suspender cables, the main cables are not replaceable. Therefore, the main cable is one of the most important components in the suspension bridge. The tensile forces of the two main cables under Tianjin earthquake are also calculated, which are shown in Figure 14.

Figure 14 shows that cables that are closer to the source have larger forces than those far from the source. In addition, the cable forces appear oscillatory when the apparent wave velocity is below 1000 m/s and then become steady when the velocity further increases.

The longitudinal shear forces at the bottoms of the three towers are studied under the El Centro earthquake to reveal the influence of various apparent wave

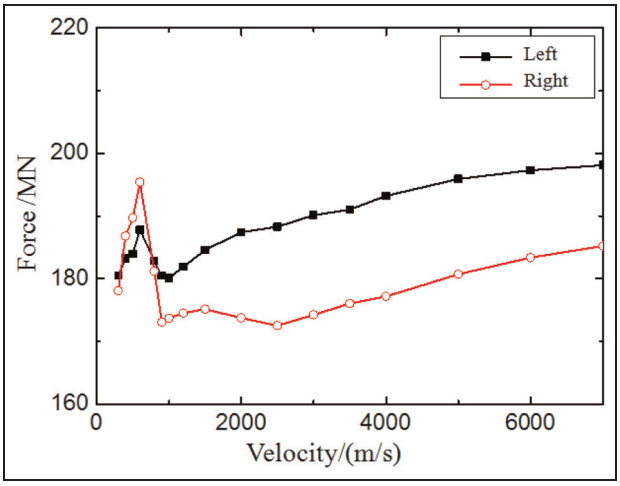

Figure 14. Influences of the velocity on force of side cables under Tianjin earthquake.

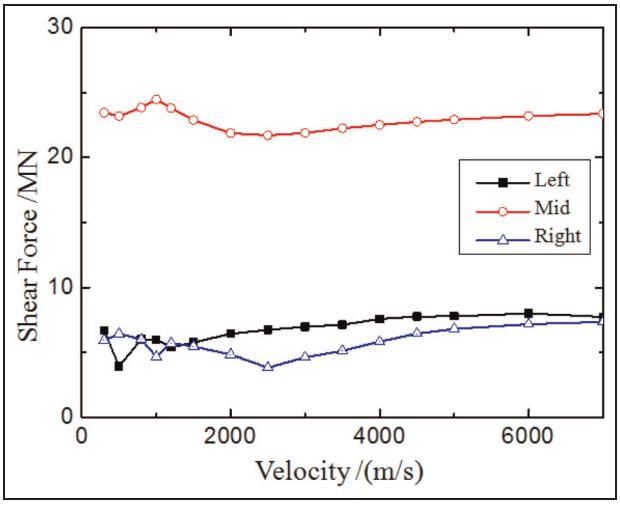

Figure 15. Influences of the velocity on longitudinal shear force at the bottom of towers under El Centro earthquake.

velocities associated with different earthquakes on the seismic responses of triple-tower suspension bridges. These shear forces are shown in Figure 15 as the apparent wave velocity increases from 300 to 7000 m/s.

Figure 15 illustrates that (1) the longitudinal shear force of the middle tower is the largest due to its large stiffness, which is consistent with the conclusions obtained under Tianjin earthquake. (2) The variation in apparent wave velocity would only cause inconspicuous effects on shear forces at bottoms of the towers under the El Centro earthquake, but has more significant influence under the Tianjin earthquake. (3) The oscillation phenomenon still exists when the apparent wave velocity is below 1500 m/s, and it disappears when the velocity is above 2500 m/s. Therefore, the effects of apparent wave velocity on the structural response are closely related to the characteristics of different earthquakes.

The above analysis shows that the structural responses appear somewhat oscillatory when the apparent wave velocity changes, showing the significant influence of apparent wave velocity. Thus, it is inappropriate to conduct calculations of traveling wave effect based on a hypothetical apparent wave velocity. The oscillatory phenomenon may be perceived as a preliminary explanation for the inhomogeneous or even contradictory conclusions mentioned in the literature review.

The characteristics of both the bridge and the seismic input are two crucial factors affecting the traveling wave effect. Selection of seismic wave which is consistent with the bridge site is especially important. Considering the uncertainty of the direction of seismic wave, the side tower with larger seismic responses should be selected for analysis during the seismic design of long-span triple-tower bridges.

Conclusion

Traveling wave effect is an important factor in the analysis of seismic response of long-span bridges. There is still no consensus about the effects of traveling wave on structures because different conclusions can be drawn under different apparent wave velocities. In addition, studies on long-span triple-tower suspension bridges are extremely limited. In this article, the state-of-the-art of the studies on the effects of traveling wave on long-span bridges is reviewed at first; Taizhou Bridge is then chosen as a numerical example to study the effects of apparent wave velocities on seismic responses of long-span triple-tower suspension bridges. Distribution characteristics of the internal force envelopes of the three towers and displacement characteristics of other typical components are given, and the influences of traveling wave effect are investigated. The conclusions are drawn as follows:

1. Although the elastic restraints made of steel stranded wires and viscous dampers are employed in Taizhou Bridge to control the longitudinal movement of the main girder, the longitudinal relative displacements between the main girder and the left side tower under Tianjin earthquake could be larger than 0.5 m, which deserves special attention during the operation of the bridge.
2. For a triple-tower suspension bridge, internal forces of components which are closer to the seismic source will be generally larger than those of components which are far from the source. The comparison of internal forces of side cables under Tianjin earthquake is a typical example. Since the direction of seismic wave propagation

is uncertain before an earthquake happens, it is necessary for engineers to take the influences of seismic wave propagation on structures into account, and the most unfavorable direction should be employed in the structural design.

3. Seismic responses of triple-tower suspension bridges considering traveling wave effect are sensitive to the spectral characteristics of seismic inputs. In this article, the longitudinal shear forces at the bottoms of towers under the El Centro earthquake and the Tianjin earthquake are different. Therefore, selection of suitable seismic input according to the characteristics of the bridge site is extremely important.
4. When apparent wave velocity is low, relative seismic responses of key components in triple-tower suspension bridges (e.g. relative displacements of the towers and the main girder, reaction forces at bottoms of the towers, internal forces of side cables) will appear oscillatory, and this trend will vanish gradually and stabilize with the increase in the velocity. Thus, proper adoption of the range of apparent wave velocity corresponding to the bridge site is crucial to the analysis results.
5. When apparent wave velocity is larger than 2500 m/s, the oscillatory nature of the structural seismic forces versus apparent wave velocity disappears, and moments and shear forces of the triple-tower suspension bridge show a rising trend with the increase in wave velocity. However, the growing trend will slow down gradually. It can be expected that the seismic responses will be the same as those from the uniform ground motion when the wave velocity is large enough. Therefore, the structural seismic responses of the bridge under uniform ground motion are generally larger than those under non-uniform ground motion.

Acknowledgements

The authors would like to thank the fruitful work provided by the Construction Commanding Department of Jiangsu Provincial Yangtze River Highway Bridge.

Declaration of conflicting interests

The authors declare that there is no conflict of interests regarding the publication of this article.

Funding

This work was supported by the National Basic Research Program of China (973 Program) (Grant No. 2015CB060000), the National Science Foundation of China (Grant Nos 51278104, 51378111, and 51438002), the Key Laboratory of Bridge Earthquake Resistance Technology of Ministry of Communications of China (Grant No. 201302), the Program for New Century Excellent Talents in University of Ministry of Education of China (Grant No. NCET-13-0128), and the Fok Ying-Tong Education Foundation for Young Teachers in the Higher Education Institutions of China (Grant No. 142007).

References

1. Newmark NM. A method of computation for structural dynamics. *J Eng Mech Div* 1959; 85: 67–94.
2. Bathe KJ and Wilson EL. Stability and accuracy analysis of direct integration methods. *Earthq Eng Struct D* 1972; 1: 283–291.
3. Li J, Spencer BF Jr, Elnashai AS, et al. Substructure hybrid simulation with multiple-support excitation. *J Eng Mech* 2012; 138: 867–876.
4. Kiureghian AD and Neuenhofer A. Response spectrum method for multi-support seismic excitations. *Earthq Eng Struct D* 1992; 21: 713–740.
5. Loh CH and Ku BD. An efficient analysis of structural response for multiple-support seismic excitations. *Eng Struct* 1995; 17: 15–26.
6. Soyluk K. Comparison of random vibration methods for multi-support seismic excitation analysis of long-span bridges. *Eng Struct* 2004; 26: 1573–1583.
7. Elnashai AS and Di Sarno L. *Fundamentals of earthquake engineering*. Chichester: John Wiley & Sons, 2008.
8. Zanardo G, Hao H and Claudio M. Seismic response of multi-span simply supported bridges to a spatially varying earthquake ground motion. *Earthq Eng Struct D* 2002; 31: 1325–1345.
9. Dumanogluid AA and Soyluk K. A stochastic analysis of long span structures subjected to spatially varying ground motions including the site-response effect. *Eng Struct* 2003; 25: 1301–1310.
10. Abdel-Ghaffar AM and Rubin LI. Suspension bridge response to multiple-support excitations. *J Eng Mech* 1982; 108: 419–435.
11. Abdel-Ghaffar AM and Rubin LI. Vertical seismic behavior of suspension bridges. *Earthq Eng Struct D* 1983; 11: 1–19.
12. Abdel-Ghaffar AM and Rubin LI. Lateral earthquake response of suspension bridges. *J Eng Mech* 1983; 109: 664–675.
13. Dumanoglu AA, Brownjohn JM and Severn RT. Seismic analysis of the Fatih Sultan Mehmet (Second Bosporus) suspension bridge. *Earthq Eng Struct D* 1992; 21: 881–906.
14. He QX and Shen ZY. Review of structural seismic analysis of travelling wave effects. *J Earthq Eng Eng Vib* 2009; 29: 50–57.
15. Pan DG, Lou ML and Fan LC. Status of seismic response analysis of long-span structures under multiple support excitations. *J Tongji Univ* 2001; 29: 1213–1219.
16. Zerva A. Spatial variation of seismic ground motions: an overview. *Appl Mech Rev* 2002; 55: 271–297.
17. Peng YH. *Research on the relation between the binds and seismic response of long-span suspension bridge and push-over analysis of the tower*. ME Thesis, Civil Engineering Department, Hunan University, Changsha, China, 2007.

18. Zembaty Z. Spatial seismic excitations and response spectra. *J Eng Technol* 2007; 44: 233–258.
19. Zembaty Z and Krenk S. Spatial seismic excitations and response spectra. *J Eng Mech* 1993; 119: 2449–2460.
20. Harichandran RS and Vanmarcke EH. Stochastic variation of earthquake ground motion in space and time. *J Eng Mech* 1986; 112: 154–174.
21. Ates S, Bayraktarb A and Dumanoglu AA. The effect of spatially varying earthquake ground motions on the stochastic response of bridges isolated with friction pendulum systems. *Soil Dyn Earthq Eng* 2006; 26: 31–44.
22. Soyluk K and Dumanoglu AA. The effects of local soil conditions and wave velocities to the stochastic response of cable-stayed bridges. In: *Proceedings of the ECAS2002 international symposium on structural and earthquake engineering*, Ankara, 14 October 2002, pp.134–141.
23. Fan LC, Wang JL and Chen W. Response characteristics of long-span cable-stayed bridges under non-uniform seismic action. *Chin J Comput Mech* 2001; 118: 358–363.
24. Wang J, Carr AJ, Cooke N, et al. The response of a 344 m long bridge to non-uniform earthquake ground motions. *Eng Struct* 2009; 31: 2554–2567.
25. Xiang HF. Earthquake response analysis of cable-stayed bridges under the action of travelling waves. *J Tongji Univ* 1983; 2: 1–9.
26. Rassem M, Ghobarah A and Heidebrecht AC. Site effects on the seismic response of a suspension bridge. *Eng Struct* 1996; 18: 363–370.
27. Wang H, Li AQ, Jiao CK, et al. Damper placement for seismic control of super-long-span suspension bridges based on the first-order optimization method. *Sci China Technol Sci* 2010; 53: 2008–2014.
28. Yoshida O, Okuda M and Moriya T. Structural characteristics and applicability of four-span suspension bridge. *J Bridge Eng* 2004; 9: 453–463.
29. Deng YL, Peng TB, Li JZ, et al. Study on dynamic characteristic and aseismic performance of a long-span triple-tower suspension bridge. *J Vib Shock* 2008; 27: 105–110.
30. Wilson EL. *Three-dimensional static and dynamic analysis of structures*. Berkeley, CA: Computers & Structures, Inc., 2002.
31. Yu HF and Zhang YC. Discussion on earthquake input method. *Eng Mech* 2009; 26: 1–6.
32. Nazmy AS and Abdel-Ghaffar AM. Effect of ground motion spatial variability on the response of cable-stayed bridges. *Earthq Eng Struct D* 1992; 21: 1–20.
33. Nazmy AS and Abdel-Ghaffar AM. Nonlinear earthquake-response analysis of long-span cable-stayed bridges: theory. *Earthq Eng Struct D* 1990; 19: 45–62.
34. Wang H, Li AQ and Hu RM. Comparison of ambient vibration response of the Runyang Suspension Bridge under skew winds with time-domain numerical predictions. *J Bridge Eng* 2011; 16: 513–526.
35. Wang H, Tao TY, Zhou R, et al. Parameter sensitivity study on flutter stability of a long-span triple-tower suspension bridge. *J Wind Eng Ind Aerod* 2014; 128: 12–21.
36. Xu Y, Ko J and Zhang W. Vibration studies of Tsing Ma suspension bridge. *J Bridge Eng* 1997; 2: 149–156.
37. Abdel-Ghaffar AM. Vibration studies and tests of a suspension bridge. *Comput Struct* 2000; 76: 787–797.
38. Erkus B, Abe M and Fujino Y. Investigation of semi-active control for seismic protection of elevated highway bridges. *Eng Struct* 2002; 24: 281–293.
39. He WL, Agrawal AK and Mahmoud K. Control of seismically excited cable-stayed bridge using resetting semiactive stiffness dampers. *J Bridge Eng* 2001; 6: 376–384.
40. Murphy TP and Collins KR. Retrofitting suspension bridges using distributed dampers. *J Struct Eng* 2004; 130: 1466–1474.